Available online www.jocpr.com

Journal of Chemical and Pharmaceutical Research, 2017, 9(10):

Research Article

ISSN : 0975-7384
CODEN(USA) : JCPRC5

Mixed Ligands Ternary Complexes of n-Acetylcysteine with Some Transition Metal Ions; Synthesis, Characterization, Biological and Antitumor Activities

Naglaa M. Mohamed, Abbas W. Salman, Sura H. Khatham*** and M. E. Moustafa***

**Chemistry Department, Faculty of Science, Benha University, Benha, Egypt, E-mail:dr.moustafa 1955@yahoo.com*

*** Chemistry Department, Faculty of Science, Wasit University, Iraq*

**** abstracted from her M.Sc. Thesis*

ABSTRACT

Nine mixed ligands complexes of Mn(II), Co(II), Ni(II), Cu(II) and Zn(II) with N-acetylcysteine (NAC) as primary ligand and six amine derivatives as secondary ligands were prepared and characterized by elemental and thermal analysis, magnetic measurements, IR and electronic absorption spectra. The study showed the formation of complexes with stiochiometric ratio NAC:M:Amine 1:1:1 and sometimes 1:1:2. The prepared complexes showed enhanced activities towered some gram positive and gram negative bacteria as well as towered Breast Carcinoma; MCF-7 cell line and Lung Carcinoma A- 549 cell lines. The optimized molecular structures of some complexes were determined using DMOL^3 program and density functional theory calculation (DFT).

Keywords: Mixed ligands complexes; N-Acetylcestiene; Antibacterial; Antitumor activities

---

INTRODUCTION

Studies on mixed ligand complexes of amine derivatives are of immense biological interest because such complexes show interesting properties like antibacterial, antifungal and anticancer [1-6]. N-acetylcysteine is an organic compound which had been approved as one of the essential medicines for basic health system by World Health Organization (WHO) [7]. It is known as a precursor for glutathione, the antioxidant which prevents formation of oxidative species in tissue [8]. Thiol group of N-acetylcysteine can prevent sulfur depletion in body [9] and also had been reported as a potential chelating agent for many metals ions [10,11]. Mixed ligand complex formation occurs widely in systems where metal ions and two or more different ligands are present [12]. It was reported early that at the physiological pH of 7.4 about 98% of copper (II) in the simulated plasma solution is present as a mixed complex of copper: histidine: cysteine, while as substantial percentage of zinc (II) was also found as a zinc: cysteine: histidine complex [13]. Mixed ligand complexes also play important role in the catalytic centers of metalloenzymes and metal activated enzymes [14], thus investigation the interaction between various transition metals and amino acids and their ternary complexes can be used as metalloenzyme models. Considering the importance of the mixed ligand complexes of amine derivatives and N-acetycysteine, this work studies the synthesis and characterization of ternary complexes of manganese (II), nickel (II), cobalt (II), copper (II) and zinc (II) with N-acetylcysteine (NAC) as primary ligand and various amine derivatives as secondary ligands.

EXPERIMENTAL SECTION

Materials

All reagents used in the present study were of the highest quality (Merck, Aldrich, Fluka or Sigma Research Laboratories) and were used without further purification. The primary ligand; *N*-acetylcysteine also known as *N*-acetyl-L-cysteine (NAC) and the secondary ligands (amine derivatives) have the following structural formula

(Figure1):

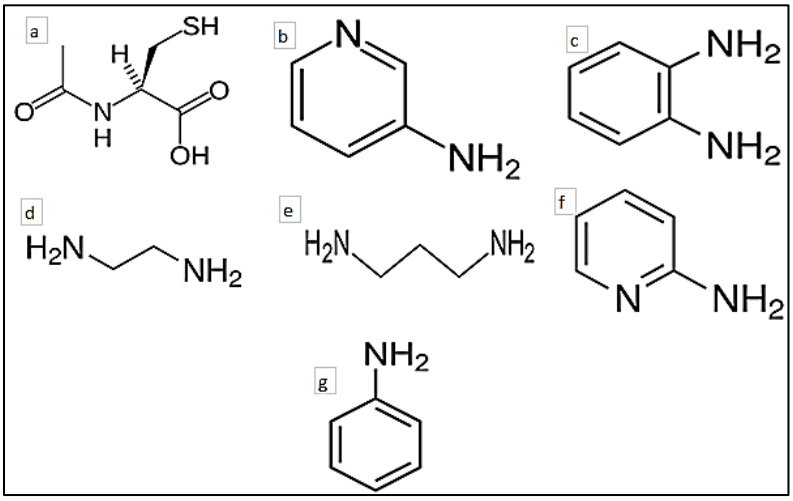

Figure 1: a. N-Acetylcysteine (NAC), b. 3-aminopyridine, (3AP), c. *o*-Phenylenediamine; (OPD) d. Ethelenediamine, (en); e. 1,3-diaminopropane, (DAP) f. 2-aminopyridine, (2AP), g. Aniline, (AN)

Preparation of the Mixed Ligands Solid Complexes

Mixed ligand Mn(II), Co(II), Ni(II), Cu(II) and Zn(II) complexes (A1-A9) were prepared from hydrated metal chloride. Aqueous solution of 1.00 mmol of metal salts was added with stirring to an ethanolic solution of 1.00 mmol of each of the secondary ligands and the mixture was refluxed for ≈3 hours. To the above mixture, an ethanolic solution of N-acetylcysteine (1.00 mmol), as primary ligand, was added. The mixture (1:1:1 molar proportion) was again refluxed in a water bath for 3 hours. The mixture was then cooled to room temperature, and the solid complexes so formed were filtered off and washed with distilled water followed by ethanol and dried under vacuum.

Physical Measurements

Elemental analysis; (C, H and N) of the mixed ligands complexes were carried out in the microanalytical centre, Cairo University, Giza, Egypt. Metal ion content (Mn, Ni, Co, Cu and Zn) was determined by EDTA titration under the appropriate conditions [15]**.** Infrared spectra were recorded as KBr disc technique. Percent transmittance was recorded against wavenumber using FT – IR spectrometer Model Nicolet is 10-thermo-scientific within the wavenumber range 4000-400 cm^{-1}. Thermogravimetric analysis; (TGA-DTA) was carried out using Shimadzu TGA – 50H thermal analyzer within the range 25 - 800°C under nitrogen atmosphere at heating rate of 10°C per minute. The electronic absorption spectra of the complexes in solid state (Nujol mull technique) were recorded on Jasco V – 530 (UV-Vis) double beam spectrophotometer (Japan) with scanning speed 400 nm/min and band width 2.0 nm using 10 mm matched quartz cell at room temperature in the range 800-200 nm. Magnetic moments were measured at room temperature using a Sherwood scientific magnetic susceptibility balance. Molar conductivities of the complexes (10^{-3} M) in DMF were obtained using a conductivity bridge YSI model 32.

Antimicrobial Screening

The antibacterial activity of some selected mixed ligands complexes toward four bacterial strains [two Gram-positive bacteria (*Streptococcus pyogenes* and *Staphylococcus epidermidis*) and two Gram -negative bacteria (*Salmonella typhi* and *Escherichia coli)]* was measured by agar well diffusion method [16]. Standard drug; Ampicillin and DMF solvent control were screened separately for their antibacterial activity. The tested compounds were dissolved in DMF which have no inhibition activity to get concentration of 100 mg/ml. A hot nutrient agar solution (20 ml) was poured into the sterilized petri dishes and allowed to attain room temperature. The seed layer medium was melted and cooled to ≈45°C with gentle shaking. The previously grown subculture was added to the seed layer medium aseptically and mixed well. It was immediately raked into the petri dishes and allowed to attain room temperature. Then wells were made with the sterile cork porer and to these wells, 50 µl in concentration of 100 mgl/ml of the tested compound was added and the plates were allowed to cool for one hour to facilitate the diffusion. The plates were incubated at 37°C for 24 hours. Antibacterial activity of the complexes was evaluated by measuring the diameter of zone of inhibition in mm. The medium with DMF as solvent was used as a negative

control whereas media with Ampicillin were screened separately for its standard antibacterial activity.

Antitumor Activity Assay

In vitro anticancer activity of selected complexes was tested against mammalian cell lines: MCF-7 cells (human breast cancer cell line) and A-549 cells (human lung carcinoma) using MTT method [17,18]. All measurements were carried out at the Regional Center for Mycology and Biotecnology, Al-Azhar University, Cairo, Egypt.

Molecular Modeling

The cluster calculations using $DMOL^3$ program [19] in materials studio package [20] which is designed for the realization of large scale density functional theory calculation (DFT) were performed to obtain the optimized molecular structure of some complexes.

RESULTS AND DISCUSSION

Elemental Analysis and Molar Conductivity

All the complexes are colored, stable in air and have high melting points. They are freely soluble in DMSO and DMF but sparingly soluble in other common organic solvents. Results of elemental analysis (Table 1) are in good agreement with the calculated values of the proposed formulae. The values reveal that the N-acetylysteine: metal: secondary ligand ratio are 1:1:1 and 1:1:2 (in some cases). The chemical composition (C, H, N and M) of the solid complexes was determined by elemental analysis. The number of water molecules attached to the metal chelates was determined by dehydration method. Based on the data given, the corresponding probable constitutional formula for the different complexes are suggested and given in Table 1. The values of molar conductivities lie within the range 29.12 - 38.47 $ohm^{-1}cm^2mol^{-1}$ indicating their ionic nature with number of ions equals two. The presence of the counter anion (Cl^-) outside the coordination sphere is confirmed by the precipitation of Cl^- as AgCl by the addition of $AgNO_3$ solution to the solubilized chelates in DMF.

Table 1: Elemental analysis and molar conductivity of themixed 2-acetyl-thiophene-amine derivatives complexes

Complex	ν_{OH}	ν_{NH2}	$\nu_{C=O}$	ν_{C-S}	δ_{NH}	δ_{OH}	ν_{M-S}	ν_{M-O}	ν_{M-N}
A1	---	3318	1593	705	1450	---	688	603	520
A2	3444	3339	1571	655	1435	1108	663	617	501
A3	3173	3105	1575	584	1385	1088	757	594	502
A4	3520	3329	1622	705	1150	1089	721	600	452
A5	3580	2986	1609	685	1192	1106	785	717	509
A6	3425	3230	1615	655	1250	1095	725	685	505
A7	3547	3330	1887	715	1241	1128	693	508	450
A8	3254	---	1588	650	---	1025	652	557	430
A9	3314	3249	1601	675	1246	996	687	610	542

*values between parentheses are found values, ** $ohm^{-1}cm^2mol^{-1}$

Thermal Analysis

The thermogravimetrical behavior of some selected solid complexes (complexes A1, A3, A4, A7, A8 and A9) was studied within the range 250-800°C under nitrogen atmosphere. Representative thermogram examples are given in Figures 2 and 3. Inspection of the TG - DT curves shows that. The mixed NAC: M: amine derivative complexes degrade thermally within the temperature range 50.05°C – 533.99°C through, more or less, three main steps.

The first step within the temperature range 50.05 -135.69°C corresponds to the removal of physically adsorbed and coordinated water molecules. This step appears, sometimes as a composite one. The percent of coordinated and number of water molecules was calculated from the inflection in the TG curve corresponding to exothermic peak on the DT curve. The unhydrated solid complex begins to decompose thermally through the second step within the range 103.74-384.00°C in which CO_2 and N_2 gases are evolved as a result of the decomposition of the amine derivative moieties representing the secondary ligand. Full thermal decomposition takes place through the third step within the temperature range 408.74-533.99°C with the evolution of SO_2 gas resulting from the thermal degradation of the N-acetylcyctein moiety leading to metal oxides and carbon as final products. The overall weight losses of the degradation steps were calculated and the metallic residues were determined. The thermogravimetric date and the assignment of different thermal degradation steps are summarized in Table 2.

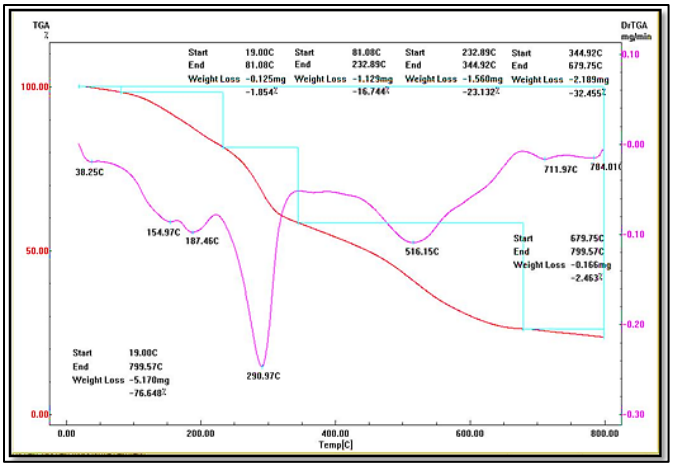

Figure 2: Thermogravimetric differential thermal analysis of complex A1

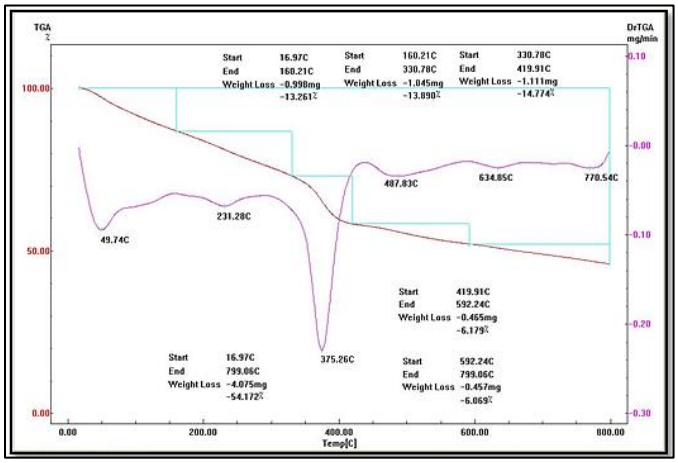

Figure 3: Thermogravimetric differential thermal analysis of complex A3

Table 2: Thermogrivemetric data for the NAC: M: Amine derivatives complexes

Complex	Temp.(°C)	Weight Loss (%)	Assignment
[Ni(NAC)(en)(H_2O)$_2$]Cl A1	61.79 147.26 251.25 416.09	*4.4* 8.99 16.92 43.25	Removal of humidity H_2O molecule, Starting decomposition of 2^{ry} ligand. Decomposition of NAC Moiety leading to NiO_2 and carbon
[Zn(NAC)(OPD)(H_2O)$_2$]Cl A3	123.97 258.92 408.74	10.9 16.54 41.15	Removal of coordinated H_2O molecule, Starting decomposition of 2^{ry} ligand. Decomposition of NAC Moiety leading to ZnO and carbon
[Ni(NAC)(2AP)$_2$(H_2O)$_2$]Cl A4	135.69 384.06 533.99	16.86 41.82 19.74	Removal of coordinated H_2O molecule Starting decomposition of 2^{ry} ligand. Decomposition of NAC Moiety leading to NiO_2 and carbon

$[Co(NAC)(AN)_2(H_2O)_2]Cl$ A7	85.68 227.73 501.9		Removal of coordinated H_2O molecule Starting decomposition of 2^{ry} ligand. Decomposition of NAC Moiety leading to CoO and carbon
$[Zn(NAC)(3AP)_2(H_2O)_2]Cl$ A8	50.05 103.74 521.7	9.42 17.44 46.08	Removal of humidity H_2O molecule, Starting decomposition of 2^{ry} ligand. Decomposition of NAC Moiety leading to ZnO and carbon
$[Ni(NAC)(An)_2(H_2O)_2]Cl$ A9	56.98 259.27 411.88		Removal of humidity H_2O molecule, Starting decomposition of 2^{ry} ligand. Decomposition of NAC Moiety leading to NiO_2 and carbon

Infrared Spectra

The assignment of the IR bands was carried out by applying a method similar to that suggested by Looker [21] according to which the spectrum was subdivided into three regions, namely; the 4000-2800, 1700-1500, 1500-1000 and 1000-625 cm^{-1}. The absorption band frequencies (cm^{-1}) are listed in Table 3 from which it can be concluded that:

The spectrum of the free N-acetylcystein ligand shows strong band at 1605 cm^{-1} and weak band at 725 cm^{-1} due to the stretching vibrations of carbonyl group ($V_{C=O}$) and V_{C-S} bonds. The latter band appears as weak one of variable intensity within the range 720-570 cm^{-1}. These two vibrational bands suffer a notable shift to lower frequencies in the spectra of complex species. This lower frequency shift is due to the delocalization of electron cloud on the oxygen and sulfur atoms as a result of donation of lone pairs of electrons to form the coordination bonds.

The IR spectra of the free amine derivatives (acting as secondary ligands), show the characteristic bands within the rang 2986 cm^{-1}- 3339 cm^{-1} due stretching vibration of the NH_2 group (V_{NH2}), while the IR spectra of complexes A4 and A8 show two strong bands at 1555 cm^{-1} and 1562 cm^{-1}, respectively due to the stretching vibration of C=N group in aromatic ring. In a similar way the vibrational spectral frequencies of these bands are shifted to lower frequency side on complex formation.

The stretching vibrations (V_{OH}) of free OH group coordinated water molecule are detected by the broad band within the range 3173-3580 cm^{-1}, while the bending mode (δ_{OH}) appears as medium – strong band within the range 996 - 1128 cm^{-1}

The far infrared region of the spectra of the metal chelates shows three new sets of bands within the regions 663-785, 557-717 and 452-520 cm^{-1} which are due to the stretching vibrations of M-S, M-O and M-N bonds, respectively. Thus, it is opvios that the primary ligand acts as monovalent bidentate and the secondary ligands act as neutral bidentate leading to SONN coordination fashion. Elemental analysis confirmed the formation of NAC : M : amine derivative complexes with steochiometric ratio 1:1:1 (or sometimes 1:1:2), accordingly the mode of bonding of such complexes is represented in Figure 4.

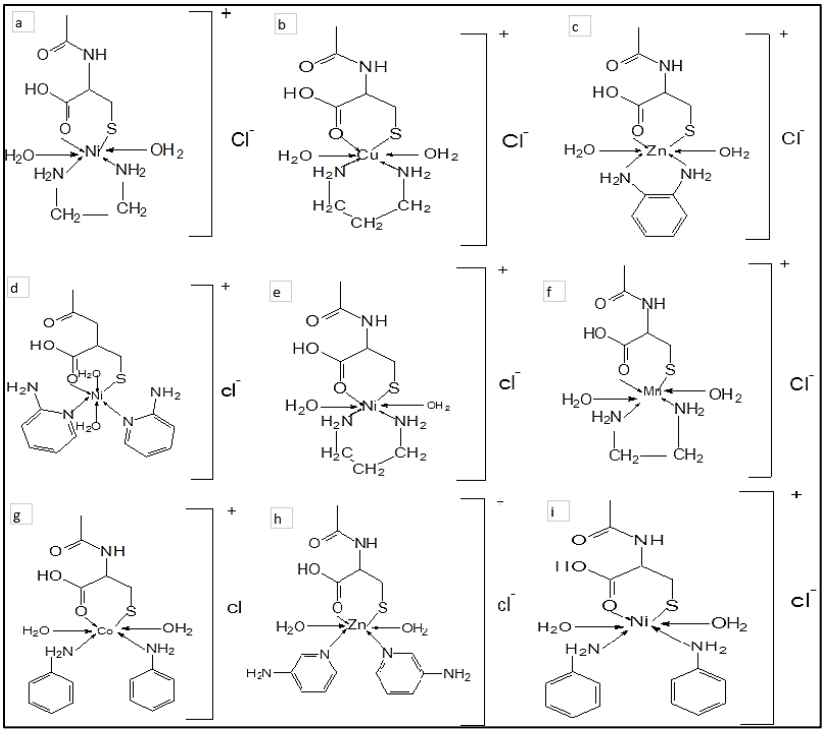

Figure 4: a)A1;[Ni(NAC)(en)$(H_2O)_2$]Cl(1:1:1), b)A2;[Cu(NAC)(DAP)$(H_2O)_2$]Cl(1:1:1), c)A3; Zn(NAC)(OPD)$(H_2O)_2$]Cl(1:1:1), d)A4;[Ni(NAC)$(2AP)_2(H_2O)_2$]Cl(1:1:2), e)A5; [Ni(NAC)(DAP)$(H_2O)_2$]Cl(1:1:1), f) A6; [Mn(NAC)(en)$(H_2O)_2$]Cl(1:1:1), g) A7; [Co(NAC)$(AN)_2(H_2O)_2$]Cl(1:1:2), h) A8; [Zn(NAC)$(3AP)_2(H_2O)_2$]Cl(1:1:2), i) A9; [Ni(NAC)$(An)_2(H_2O)_2$]Cl(1:1:2)

Table 3: IR vibrational frequencies (cm-1) of some function groups of NAC: M: amine derivative complexes

Complex	V_{OH}	V_{NH2}	$V_{C=O}$	V_{C-S}	δ_{NH}	δ_{OH}	V_{M-S}	V_{M-O}	V_{M-N}
A1	---	3318	1593	705	1450	---	688	603	520
A2	3444	3339	1571	655	1435	1108	663	617	501
A3	3173	3105	1575	584	1385	1088	757	594	502
A4	3520	3329	1622	705	1150	1089	721	600	452
A5	3580	2986	1609	685	1192	1106	785	717	509
A6	3425	3230	1615	655	1250	1095	725	685	505
A7	3547	3330	1887	715	1241	1128	693	508	450
A8	3254	---	1588	650	---	1025	652	557	430
A9	3314	3249	1601	675	1246	996	687	610	542

Magnetic Susceptibility and Electronic Spectra

Magnetic susceptibility measurements of the solid complexes, at room temperature, were performed. The values exhibit paramagnetism for Mn(II), Ni(II) Co(II) and Cu(II) complexes and diamagnetism for Zn(II) complexes. The μ_{eff} values, term symbols and ground state symbols are listed in Table 4.

Electronic Absorption Spectra

The electronic absorption spectra of the complexes are studied in solid state (using Nujol mull technique) and compared to those of the free ligands.

- For Mn(II) and other d^5 cases, the ground state is ^6S and higher states include, ^4G, ^4D, ^4P ^4F etc. It is expected that since there are no spin-allowed transitions possible, the electronic spectrum should only contain very weak bands. So, by amplifying the signal and using concentrated solutions, a number of weak peaks can be seen and assigned as $^6A_{1g} \rightarrow {}^4T_{1g}(4G)$, $\rightarrow {}^4E_g(4D)$, $\rightarrow {}^4T_{1g}(4P)$ and $\rightarrow {}^4E_g(G)$.
- Cobalt (II) is a d^7 ion with $t_{2g}{}^5e_g{}^2$ configuration. From the high spin T-S diagram, the ground state is $^4T_{1g(F)}$ and the spin multiplicity is a quartet. The diagram shows that there are three quartet excited state; $^4T_{2g}(F)$, $^4T_{1g}(P)$ and $^4A_{2g}(F)$, so, the (d-d) electronic transition will be of the type $^4T_{1g(F)} \rightarrow {}^4T_{1g(P)}$ (V_3), $^4T_{1g(F)} \rightarrow {}^4A_{2g(F)}$ (V_1) and $^4T_{1g(F)} \rightarrow {}^4T_{2g(F)}$ (V_2), respectively [22].

The electronic spectra of Ni (II) (d^8 configuration) complexes show the three spin allowed bands (Table 5) which are assigned to electronic transitions of the type $^3A_{2g(F)} \rightarrow {}^3T_{1g(P)}$, $^3A_{2g(F)} \rightarrow {}^3T_{1g(F)}$ and $^3A_{2g(F)} \rightarrow {}^3T_{2g(F)}$ respectively. Copper (II) complexes show two spin allowed transition bands due to the $^2a_{1g(D)} \rightarrow {}^2b_{1g(D)}$ and $^2e_{g(D)} \rightarrow {}^2b_{1g(D)}$ transitions. The broadness of the band could be attributed to the overlapping of several bands as a result of strong Jahn-Teller distortion expected in a d^9 ion [23**].** Finally, the electronic configuration of Zn (II) complexes (d^{10}) confirms the absence of any d→d transitions. The absorption bands in its spectra are due to n→π* or CT interaction (Zn → L). The spectral data are fully assigned in Table 5 and shown graphically in Figure 5.

Table 4: Magnetic properties of the mixed ligands complexes

Complex	d^n	Electronic configuration	Term symbol	Ground State	μ_{eff} (BM)	
					Found	Theor.
[Ni(NAC)(en)]Cl_2	d^8	$t_{2g}^6e_g^2$	^3F	$^3A_{2g}$	2.85	2.828
[Cu(NAC) (DAP)$(H_2O)_2$]Cl	d^9	$t_{2g}^6e_g^3$	^2D	^2E_g	1.74	1.732
[Zn(NAC) (OPD)$(H_2O)_2$]Cl	d^{10}	$t_{2g}^6e_g^4$	---	---	Dia	Dia
[Ni(NAC)$(2AP)_2$ $(H_2O)_2$]Cl	d^8	$t_{2g}^6e_g^2$	^3F	$^3A_{2g}$	2.88	2.828
[Ni(NAC)(DAP) $(H_2O)_2$]Cl	d^8	$t_{2g}^6e_g^2$	^3F	$^3A_{2g}$	2.92	2.828
[Mn(NAC)(en)]Cl	d^5	$t_{2g}^3e_g^2$		$^6A_{1g}$(S		
[Co(NAC)$(AN)_2$ $(H_2O)_2$]Cl	d^7	$t_{2g}^5e_g^2$			4.18	3.88-5.20
[Zn(NAC)$(3AP)_2$ $(H_2O)_2$]Cl	d^{10}	$t_{2g}^6e_g^4$	---	---	Dia	Dia
[Ni(NAC)$(An)_2$ $(H_2O)_2$]Cl	d^8	$t_{2g}^6e_g^2$	^3F	$^3A_{2g}$	2.87	2.828

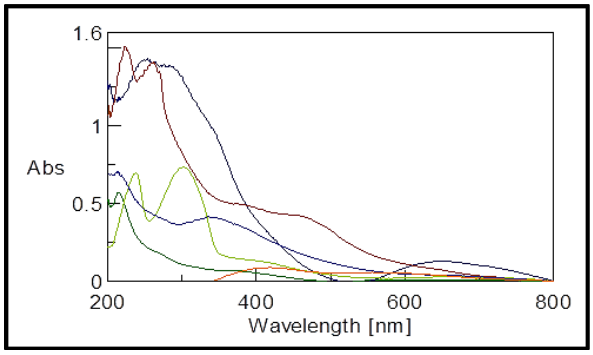

Figure 5: Electronic absorption spectra of complexes in Nujol Mull

Biological Activity and Antitumor Activity

The antimicrobial activity of some mixed ligands complexes (complexes A2, A4, A6, A7, A8 and A9) is tested against representatives of Gram – positive bacteria (*Streptococcus pyogenes* and *Staphylococcus epidermidis*) and Gram – negative bacteria (*Salmonella typhi* and *Escherichia coli)*. Standard drug; Ampicillin and DMF solvent control were screened separately for their antibacterial activity. The antibacterial results (Table 6) suggest that the mixed ligands complexes show a moderate activity against the tested organisms compared to Ampicillin taken as a standard drug. Also, percent Activity Index data show that majority of complexes have higher activity.

Increased activity on metal chelation can be explained on the basis of Overtone's concept [24] and the Tweedy's theory [25], according to which chelation reduces the polarity of the ligand due to partial sharing of its negative charge with the metal, favouring transportation of the complexes across the lipid layer of the cell membrane. The positive results suggested the very diffusion of the complexes into the bacterial cells and were able to kill the bacterium as indicated by the zones of inhibition of bacterial growth. On the other hand, the negative results can be

attributed either to the inability of the complexes to diffuse into bacteria cell membranes and hence unable to interfere with its biological activity or they can diffuse but inactivated by unknown cellular mechanism.

Table 5: Electronic absorption spectra of the mixed ligands complexes in Nojol mull

Complex	Nojol mull		Assignment	Term symbole	Ground state
	λ_{max} (nm)	Wave Number*			
[Ni(NAC)(en)]Cl_2	215 258 370	46511.6 38759.7 27027.0	$^3A_{2g(F)} \rightarrow {}^3T_{1g(P)}(\nu_3)$ $\rightarrow {}^3T_{1g(F)}(\nu_2)$ $\rightarrow {}^3T_{2g(F)}(\nu_1)$	^3F	$^3A_{2g}$
[Cu(NAC)(DAP)$(H_2O)_2$]Cl	252 286 652	39682.5 34965.0 15337.4	$^2a_{1g(D)} \rightarrow {}^2b_{1g(D)}$ $^2e_{g(D)} \rightarrow {}^2b_{1g(D)}$	^2D	^2E_g
[Zn(NAC)(OPD)$(H_2O)_2$]Cl	224 261 471 649	44642.9 38314.2 21231.4 15408.3	π-π^* π-π^* n—π^* CT	----	---
[Ni(NAC)(2AP)$_2$ $(H_2O)_2$]Cl	238 301 403sh 663w	42016.8 33222.3 24813.9 15083.0	$^3A_{2g(F)} \rightarrow {}^3T_{1g(P)}(\nu_3)$ $\rightarrow {}^3T_{1g(F)}(\nu_2)$ $\rightarrow {}^3T_{2g(F)}(\nu_1)$	^3F	$^3A_{2g}$
[Ni(NAC)(DAP)$(H_2O)_2$]Cl	215 343 655	46511.6 29154.5 15267.2	$^3A_{2g(F)} \rightarrow {}^3T_{1g(P)}(\nu_3)$ $\rightarrow {}^3T_{1g(F)}(\nu_2)$ $\rightarrow {}^3T_{2g(F)}(\nu_1)$	^3F	$^3A_{2g}$
[Mn(NAC)(en)]Cl	414 573 730w	24154.6 17452.0 13698.6	$^6A_{1g}(S) \rightarrow {}^4T_{1g}(G)$, $\rightarrow {}^4T_{2g}(G)$a $\rightarrow {}^4E_g$,	$^6S_{5/2}$	$^6A_{1g}(S)$
[Co(NAC)(AN)$_2$ $(H_2O)_2$]Cl	204 419 706w	49019.6 23866.3 14164.3	$^4T_{1g(F)} \rightarrow {}^4T_{1g(P)}(\nu_3)$, $^4T_{1g(F)} \rightarrow {}^4A_{2g(F)}(\nu_1)$ and $^4T_{1g(F)} \rightarrow {}^4T_{2g(F)}(\nu_2)$		$^4T_{1g(F)}$
[Zn(NAC)(3AP)$_2$ $(H_2O)_2$]Cl	232 283 330sh	43103.4 35335.6 30303.0	π-π^* n—π^* CT	------	------
[Ni(NAC)(An)$_2$ $(H_2O)_2$]Cl	262br 351 424sh 706br	38167.9 28490.0 23584.9 14164.3	$^3A_{2g(F)} \rightarrow {}^3T_{1g(P)}(\nu_3)$ $\rightarrow {}^3T_{1g(F)}(\nu_2)$ $\rightarrow {}^3T_{2g(F)}(\nu_1)$	^3F	$^3A_{2g}$

Table 6: Antibacterial activities of some mixed ligands complexes in terms of inhibition zone diameter (mm) and % activity index

Complex	Gram-negative				Gram-positive			
	S. typhi		*E.coli*		*S. epidermidis*		*S. pyogenes*	
	Inh. Zone(mm)	% Ac.Ind	Inh. Zone(mm)	% Ac.Ind	Inh. Zone(mm)	% Ac.Ind	Inh. Zone(mm)	% Ac.Ind
Control	15	100	30	100	20	100	24	100
A2	15	100	26	86.67	20	100	23	95.83
A4	13	86.67	22	73.33	15	75	13	54.17
A6	20	133.33	22	73.33	18	90	12	50
A7	20	133.33	21	70	24	120	18	75
A8	23	153.33	26	86.67	25	125	24	100
A9	20	133.33	26	86.67	20	100	12	50

The cytotoxic activities of some selected mixed ligands complexes *viz.*; A2 (N-acetylcestein: Cu: 1,3-diaminopropane), A4 (N- acetylgystein :Ni:2-aminopyridine) and B3 (2- acetylthiophene :Cu:o-phenelenediamine)

complexes were tested against Breast Carcinoma; MCF-7 cell line and Lung Carcinoma A- 549 cell lines. The number of viable cells and the percentage of viability were calculated as:

$$(1 - \frac{ODt}{ODc}) \times 100$$

Where, ODt is the mean optical density of the wells treated with the tested samples and ODc is the mean optical density of the untreated cells. The relation between surviving cells and drug concentration is plotted to get the survival curve of each tumor cell line after treatment with the mixed ligands complexes. The 50% inhibitory concentration (IC_{50}), (the concentration required to cause toxic effect in 50% of intact cells), was estimated from graphic plots of the dose response curve for each concentration. The results are represented graphically in Figures 6 and 7 and the lethal concentrations (IC_{50}) values are listed in Table 7.

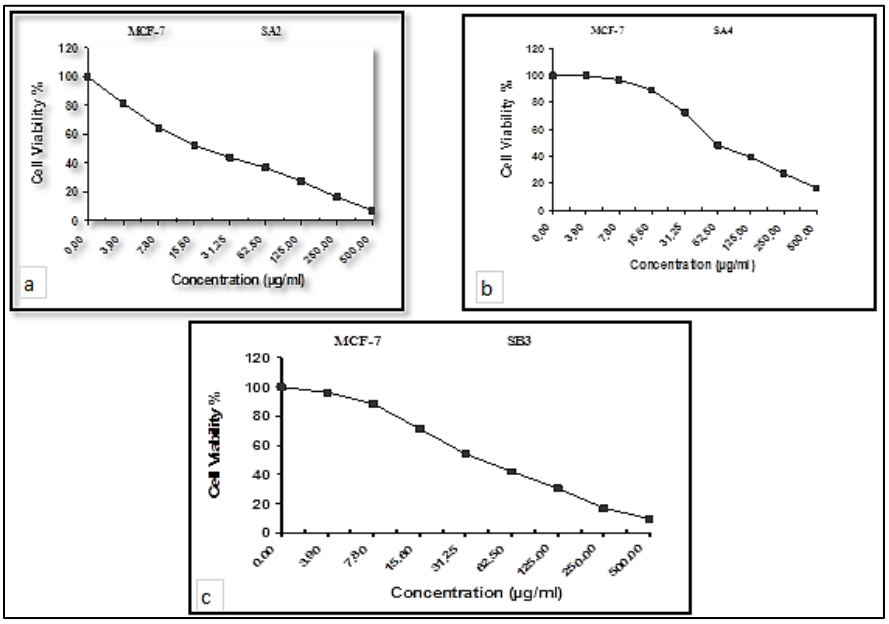

Figure 6: Cytotoxicity effect of A2, A4 and B3 complexes against MCF - 7 cell line

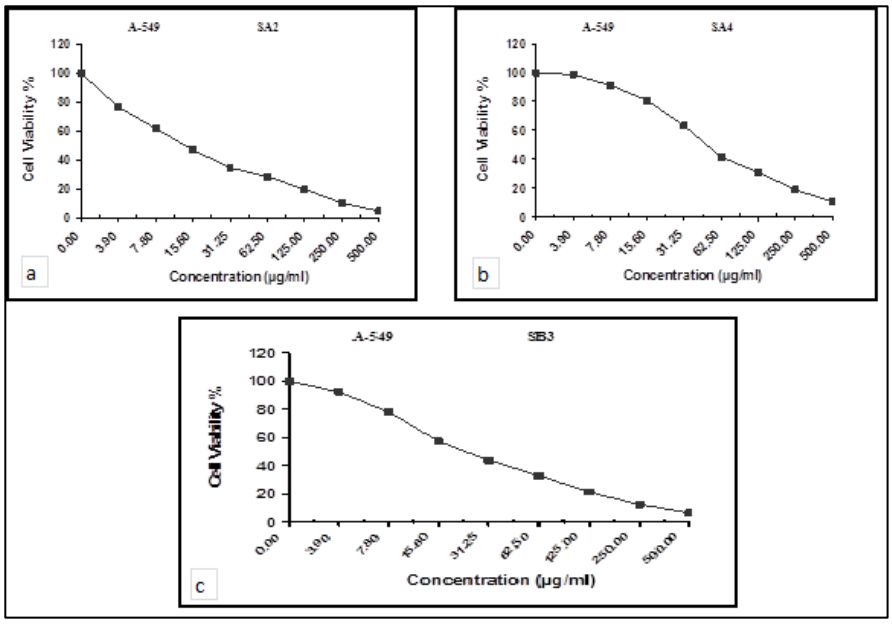

Figure 7: Cytotoxicity effect of A2, A4 and B3 complex against A - 549 cell line

Inspection of the results obtained for cytotoxcity effect (Table 7) shows that the complex A2 is the most effective to both Breast Carcinoma and Lung Carcinoma followed by the complex B3 (mixed copper complexes) and finally

SA4 (nickel complex). So, copper ion is more effective than nickel ion and is considered to have moderate activity, while nickel ion is of weak activity. The enhanced activity of metal complexes may be attributed to the increase in conjugation in the ligand moiety takes place in complexation process [26,27].

Table 7: Lethal concentration (IC50) of the mixed ligand complexes SA2, SA4 and SB3 on MCF – 7 and A – 549 cell lines

Complex	Formula	IC_{50} (µg/ml)	
		MCF - 7	A - 549
A2	$[Cu(AcTH)(DAP)(H_2O)_2]Cl_2$	19.9	13.9
A4	$[Ni(AcTH)(2AP)_2(H_2O)_2]Cl_2$	60.1	50.3
B3	$[Cu(NAC)(OPD)(H_2O)_2]Cl$	41.7	24.0

Molecular Modeling

The optimized molecular structures of some selected complexes were determined (Schemes 1-3) using DMOL[3] program and the density function theory (DFT). The calculation of bond lengths and bond angles showed that the bond distances of the functional groups participated in complex formation become longer because the formation of M-O bond makes it weaker. Also, the bond angles are quite near to an octahedral geometry predicting the d^2sp^3 or sp^3d^2 hybridization.

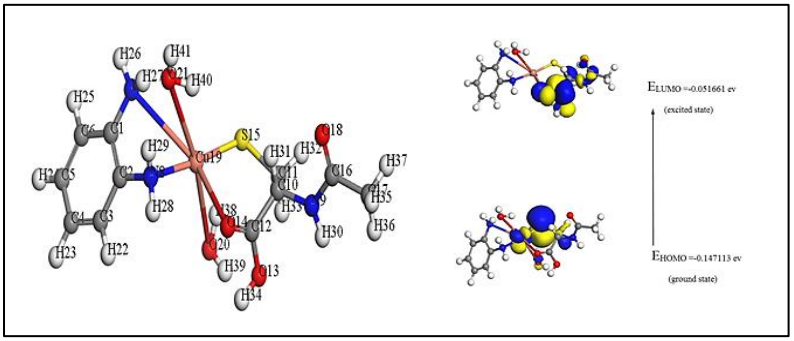

Scheme 1: Optimized molecular structure, HOMO and LOMO of the complex NAC: Cu: OPD

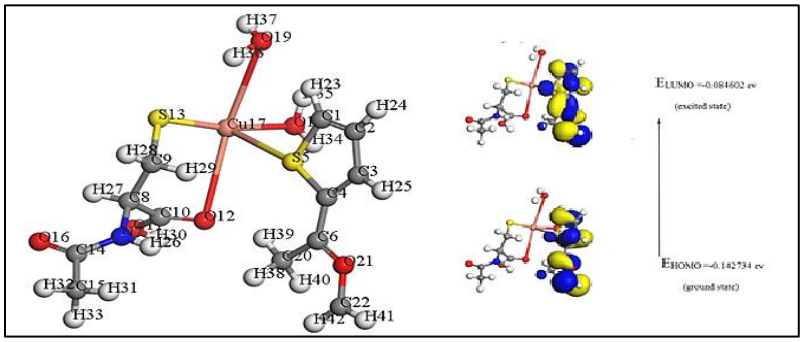

Scheme 2: Optimized molecular structure, HOMO and LOMO of the complex NAC: Cu: DAP

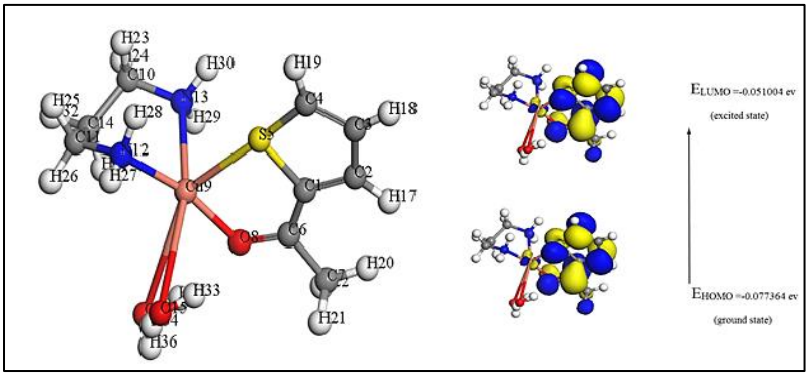

Scheme 3: Optimized molecular structure, HOMO and LOMO of the complex NAC: Co: AN

CONCLUSION

The prepared complexes showed enhanced activities towered some gram positive and gram negative bacteria as well as towered Breast Carcinoma; MCF-7 cell line and Lung Carcinoma A- 549 cell lines. The optimized molecular structures of some complexes were determined using DMOL3 program and density functional theory calculation (DFT).

REFERENCES

[1] S Quyoom**.** *Res J Chem Sci*. **2014**, 4(3), 32-35.
[2] S Ali; KE Zahan; M Haque; A Alim; M Alam. *Int J Mat Sci Appl*. **2009**, 4(4), 225-228.
[3] P Subbaraj; A Ramu; N Raman; J Dharmaraja. *Inter J Pharm Sci*. **2015**, 5(1), 839-851.
[4] U Dhusiya; S Gautam; S Chandra; S Agrawal. *J Pharm Chem Biolog Sci*. **2016**, 4(1), 1-12
[5] DA Martins; LR Gouvea; GSV Muniz; SRW Louro; DGJ Batista. *Bioinorg Chem Appl*. **2016**, Article ID 5027404, 11.
[6] AR Pramanik; AR Harun; DD Paul; PC Mondal. *J Molec Struc*. **2016**, 1059, 309-319.
[7] YTD Nguyen; SP Santoso; Yi H Ju. *Chem Pharm Bull*. **2016**, 64(11), 1560-1569.
[8] Word Health Organization "Model List Essential Medicines" WHO 15, **2007**.
[9] A Pompella; A Visvikis; A Padicchi; V DeTata; AF Casini. *Biochem Pharmacal*. **2003**, 66, 1499-1503.
[10] A Muhhamad; GS Rubina; N Amina; S Ishrat; AS Danish. *Asian J Chem*. **2015**, 27 (11), 3988-3992 .
[11] KA Taksande; DR Rautb; DM Choudharyc. *The Electronic J Chem*. **2015,** 7(4).
[12] AJ Alabdali; FM Ibrahim. *J Appl Chem*. **2014,** 6(6), 60-63.
[13] RMN Kumar; KS Prasad; N Prasad. *Chem Sci Trans*. **2015**, 4(3), 677-681.
[14] S Koç; DA Köse; E Avcı. *Euro Chem Bull*. **2016**, 5(4).
[15] Ponvel; P Athappan. *J Inorg Biochem*. **2005**, 99(3), 669-676.
[16] AI Vogel. A Text Book of Quantitative Inorganic Analysis, Longmans, London, **1994**.
[17] I Ahmad; AZ Beg. *J Ethanopharmacol*. **2001**, 74, 113-123.
[18] T Mosmann. *J Imn Methods*. **1983**, 65, 55-63.
[19] SM Gomha; SM Riyadh; E A Mahmmoud; MM Alaasser. *Hetercycles*. **2015**, 91(6), 1227-1243.
[20] B Delley. *Phys Rev B Condens Matter*. **2002**, 66, 15.
[21] Materials Studio, Accelrys software Inc San Diego, USA, **2011**.
[22] H Looker. *I Org Chem*. **1962**, 27, 361.
[23] NN Greenwood; Aearnshaw. Chemistry of the Elements. 1st Edition, Pergamon Press, Oxford, **1984**.
[24] SA Shaker; Y Farina; S Mahmoud; M Eskender. *ARPN J Eng Appl Sci*. **2009**, 4(9).
[25] N Dharamraj; P Viswanathamurthi; K Natrajan. *Trans Met Chem*. **2011,** 26, 105-109.
[26] BG Tweedy. *Phytopathol*. **1964**, 55, 910-917.
[27] HA El-oraey; AA Serag; El Din. *Molec Biomol Spectroscopy*. **2014**, 132, 663-671.